A Tumor-suppressive Molecular Axis EP300/circRERE/miR-6837-3p/MAVS Activates Type I IFN Pathway and Antitumor Immunity to Suppress Colorectal Cancer

Nan Ding[1,2], A-Bin You[1,2], Hu Yang[1], Guo-Sheng Hu[3,4], Chun-Ping Lai[1,2], Wen Liu[3,4], and Feng Ye[1,2]

ABSTRACT

Purpose: The oncogenic role of circular RNAs (circRNA) has been well studied in cancers including colorectal cancer. However, tumor-suppressive circRNAs and the mechanism through which they exert their antitumor effects remain largely unknown. We aim to find out the critical tumor-suppressive circRNAs and their possibility to serve as gene therapy targets.

Experimental Design: circRNA sequencing, gain-of-function and loss-of-function experiments, and transcriptomic analysis were performed to find tumor-suppressive and antitumor immunity effects of circRERE. Molecular biology experiments were conducted for mechanism exploration. Finally, we conducted adeno-associated virus (AAV) to deliver circRERE (circRERE-AAV) and evaluated circRERE-AAV alone and in combination with anti-PD-1 antibody in C57BL/6J mice bearing subcutaneous MC38 tumors.

Results: circRERE is lowly expressed in colorectal cancer. Overexpression of circRERE inhibits the malignant behaviors of colorectal cancer *in vitro* and *in vivo*, while knockdown exhibits the opposite effects. The expression of circRERE is regulated by EP300, a histone acetyltransferase downregulated in colorectal cancer as well. Mechanistically, circRERE acts as a competitive endogenous RNA to sponge miR-6837-3p to upregulate MAVS expression, thereby activating type I IFN signaling and promoting antitumor immunity. Delivery of circRERE-AAV elicits significant antitumor effects, and combination treatment with circRERE-AAV and anti-PD-1 antibody exhibits synergistic effects on tumor growth in preclinical models of colorectal cancer.

Conclusions: These results uncover modulatory axis constituting of EP300/circRERE/miR-6837-3p/MAVS and its essential roles in antitumor immunity, and demonstrate that circRERE-AAV might represent a new therapeutic avenue to prime immune responses and boost the effects of immunotherapy in clinic.

Introduction

In the global cancer report in 2020, colorectal cancer ranked the third and second among malignant tumors in terms of incidence and mortality, respectively (1). Even though the diagnosis and treatment have improved significantly, the majority of patients with colorectal cancer are diagnosed at an advanced stage, and therefore therapeutic options remain limited. In recent years, immunotherapy, especially immune checkpoint inhibitors (ICI), has brought hope to a certain number of patients with cancer. However, a large number of patients with colorectal cancer are not sensitive to immunotherapy. Therefore, new therapeutic approaches are in urgent need to improve the effectiveness of immunotherapy in treating colorectal cancer. Circular RNAs (circRNA), a new type of noncoding RNAs, possess a closed-loop structure without 5′ and 3′ ends to prevent their hydrolysis by exonucleases. circRNAs have been found to play critical roles in the occurrence, metastasis, and drug resistance of cancer cells through a variety of mechanisms including miRNA sponge, RNA-binding proteins scaffold, and microprotein (2–8). circRNAs are potential biomarkers for the diagnosis, treatment, and prognosis of cancers. A large number of dysregulated circRNAs have been identified and investigated in colorectal cancer (9–11). And there is a close correlation between circRNAs and antitumor immunity. Hsa_circ_0020397 induces the expression of TERT (telomerase reverse transcriptase) and PD-L1 by binding and inhibiting the activity of miR-138, thereby promoting immune escape in colorectal cancer (12). circ-0000977/miR-153/HIF1α axis regulates HIF1α-mediated immune escape of pancreatic cancer cells by inhibiting natural killer (NK)-cell killing activity (13). circARSP91 interacts with the *ULBP1* promoter region and recruits RNA polymerase II to enhance the expression of *ULBP1* gene, thus assisting NK cells to recognize and attack target tumor cells (14). circNDUFB2 was shown to be recognized by RIG-I to activate the RIG-I-MAVS signaling cascade and recruit immune cells to the tumor microenvironment (15). circRNAs are involved in almost all critical processes of tumor immunity through sponging miRNAs to regulate specific mRNAs or function as potential tumor antigens (16). Most of these circRNAs are reported to be oncogenic, while circRNAs that are tumor-suppressive are rarely reported. Furthermore, it remains largely unknown how these circRNAs exert antitumor effects.

The RIG-I-MAVS pathway is a natural immune shield against viral infections (17). RIG-I–like receptors (RLR), including RIG-I, MDA5, and LGP2, are a series of cytoplasmic RNA helicases that detect various viral RNAs accumulated during viral infection or replication (18, 19). MAVS is the core adaptor protein of RLR signal transduction. Activation of MAVS leads to the activation of interferon-regulatory factor

[1]Department of Medical Oncology, Xiamen Key Laboratory of Antitumor Drug Transformation Research, the First Affiliated Hospital of Xiamen University, School of Medicine, Xiamen University, Xiamen, P.R. China. [2]The Third Clinical Medical College, Fujian Medical University, Fuzhou, P.R. China. [3]State Key Laboratory of Cellular Stress Biology, School of Pharmaceutical Sciences, Xiamen University, Xiamen, P.R. China. [4]Fujian Provincial Key Laboratory of Innovative Drug Target Research, School of Pharmaceutical Sciences, Xiamen University, Xiamen, P.R. China.

N. Ding and A.-B. You contributed equally to this article.

Corresponding Authors: Feng Ye, First Affiliated Hospital of Xiamen University, Xiamen 361003, P.R. China. Phone: 8618-3592-91803; E-mail: yefengdoctor@xmu.edu.cn; and Wen Liu, w2liu@xmu.edu.cn

Clin Cancer Res 2023;XX:XX–XX

doi: 10.1158/1078-0432.CCR-22-3836

Translational Relevance

Over the past few years, immunotherapy is considered an innovation and has become a trend in the field of tumor treatment. However, for advanced colorectal cancer, only a small portion of patients (about 5%) could benefit from it. How to turn these "cold tumors" into "hot tumors" is of great significance. Priming the immune response might be a potential method for sensitizing the effect of immunotherapy. Our study found out a tumor-suppressive molecular axis EP300/circRERE/miR-6837-3p/MAVS that could activate type I IFN pathway and antitumor immunity. Delivery of circRERE by adeno-associated virus (circRERE-AAV) elicits significant antitumor effects, and combination treatment with circRere-AAV and anti-PD-1 antibody exhibits synergistic effects on tumor growth in preclinical models of colorectal cancer. These results demonstrate that circRERE-AAV might represent a new therapeutic avenue to prime immune responses and boost the effects of immunotherapy in clinic.

3/7 (IRF3/7) and NFκB, thus inducing type I IFN and other proinflammatory cytokines (20, 21). Subsequently, type I IFN binds to the IFNAR complex (composed of IFNAR1 and IFNAR2) to initiate the JAK/STAT downstream pathway and promote the transcription of interferon-stimulated genes (ISG), thereby priming the immune response of the host cells (22, 23). The activation of type I IFN signaling pathway is thought to be critical for improving the therapeutic effects of ICIs.

In this study, we reported that an EP300-regulated, poorly expressed circRNA, circRERE, positively regulates the expression of MAVS through sponging miR-6837–3p, thereby activating type I IFN signaling pathway to prime immune responses. Accordingly, injection of adeno-associated virus (AAV)-expressing circRERE improves the therapeutic effect of ICIs such as anti-PD-1 antibody in colorectal cancer tumor suppression.

Materials and Methods

Clinical specimens and cell culture

Colorectal cancer and the matched normal tissues were collected from patients with colorectal cancer who accepted surgery at the First Affiliated Hospital of Xiamen University (Xiamen, P.R. China). All clinical specimens were put into liquid nitrogen after surgery and sorted at −80°C until use. The study with informed consent was approved by the committee of the First Affiliated Hospital of Xiamen University (Xiamen, P.R. China) and conducted according to the Helsinki Declaration. And we confirm that all the patients provided written informed consent.

All cell lines except MC38 (RRID:CVCL_B288) were kindly provided by Professor Da-Jun Deng. MC38 was kindly provided by Professor Qin Lin. All cells were authenticated by short tandem repeat profiling by Beijing JianLian Genes Technology Co. before they were used in this study. HCT116 (RRID:CVCL_0291) and LoVo (RRID:CVCL_0399) cell lines were cultured in RPMI1640, while RKO (RRID:CVCL_0504), DLD1 (RRID:CVCL_0248), HEK293T (RRID:CVCL_0063), and MC38 were cultured in DMEM. The medium was supplemented with 10% FBS (BI) at 37°C in a humidified incubator with 5% CO_2. It was no more than 1 month between collection or thawing and use in the described experiments.

Gene knockdown and overexpression

siRNAs, miRNA mimics, and miRNA inhibitors were synthesized by RiboBio. Short hairpin RNAs (shRNA) targeting the junction of human and murine circRERE were constructed in lentiviral pLKO.1 vector. circRERE was cloned into the lentiviral expression vector pLO5-ciR (Gysey Biotechnology). Human and murine circRERE were cloned [redacted] Single-guide RNA (sgRNA) targeting EP300 gene promoter was designed and cloned into the pLV-hU6-CMV-NLS-dCas9-VP64-T2A-Puro vector to activate endogenous *EP300* transcription. All the sequences are presented in Supplementary Table S1.

Colorectal cancer cells were seeded in 6-cm plates. When they reached a confluence of 60%–80%, they were transfected with siRNA (20 μmol/L, 5 μL) or vectors (1.5 μg/well) with Lipofectamine 2000 (Invitrogen). Cells were used after 48 hours. Lentivirus packaging was done using packaging vectors pMDL, VSVG, and REV at a ratio of 10:5:3:2 as described previously (24).

Cell proliferation and colony formation assays

For cell proliferation, 1–2 × 10^3 cells were plated into 96-well plates in triplicates and subjected to treatments. Viable cells were measured by CCK8 kit (meilunbio) by Microplate Reader (Tecan) for 4–5 days.

For cell colony formation assay, 0.5–1 × 10^3 cells were seeded in 6-well plates, and the culture medium was replaced twice a week for about 10–20 days. Cells were then fixed with 100% methyl alcohol and stained with 0.1% crystal violet.

RNA extraction and qRT-PCR

Total RNA was extracted according to the protocol of Ultrapure RNA kit (Com Win). A total of 1 μg total RNA was needed for reverse transcription by GoScript Reverse Transcription Mix (Promega). Hieff qPCR SYBR Green Master Mix (Yeasen) was used to amplify the cDNA samples using Q6 real-time fluorescence quantitative PCR instrument. The classical $\Delta\Delta C_t$ method was used to calculate the relative expression levels of the target genes. C_t values were normalized to the GAPDH gene as a cDNA loading control, and changes were calculated relative to controls. All primers used are listed in Supplementary Table S2.

circRNA sequencing and RNA sequencing

Total RNA extracted from three pairs of colorectal cancer and the adjacent normal tissues after removal of genomic DNA using DNase I was digested with RNase R (Epicentre) at 37°C for 1 hour. Next-generation sequencing was performed by an Illumina HiSeq instrument according to the manufacturer's instructions (Illumina) by Amogene. CIRI2.pl was used to predict circRNA, and CIRI-full was used to predict full-length circRNAs.

For RNA sequencing (RNA-seq), HCT116 and RKO cells were transfected with control siRNA (siNC) or siRNA specifically targeting RERE (sicircRERE). After 48 hours, these cells were collected for RNA extraction. A total of 3 μg RNA per sample was used as input material for RNA-seq library preparations using NEBNext Ultra II RNA Library Prep Kit for Illumina (NEB, E7760). Paired-end sequencing was performed on the Illumina HiSeq 3000 platform at Amogene Biotech Co., Ltd. The read length used was 150 bp, and Paired-end clean reads were aligned to the reference genome using STAR V20201.

The circRERE-regulated significantly differentially expressed mRNAs were identified by evaluating the fold changes (FC) in gene FPKM (fragments per kilobase per million mapped reads) values between siNC and sicircRERE-transfected cells (with FC > 1.2 and $q < 0.05$ indicating a significant difference). Box plots were generated by R software and

significance was determined using Student *t* test. Heat maps and volcano plot were visualized using Java TreeView81 or R software.

Competitive endogenous RNA network analysis

To construct competitive endogenous RNA (ceRNA) network, miRNAs that could bind to circRERE and MAVS were predicted by three independent algorithms, miRanda (sequence align score, −sc150; ref. 25), RNAhybrid (minimal free energy, −e −23; ref. 26), and TarPmiR (probability of target site, −p 0.8; ref. 27) based on miRBase.

Chromatin isolation by RNA purification

Normal HCT116 cells (2×10^7 cells) were cross-linked with 1% glutaraldehyde solution and then lysed (50 mmol/L Tris-Cl, pH 7.0, 10 mmol/L EDTA, pH 8.0, 1% SDS, 1× protease inhibitor cocktail, and RNase). Chromatin DNA was sheared by sonication. Biotin-labeled probes targeting circRERE (RiboBio) and negative control (NC) probes were added to the above cell lysates after sonication and kept at 37°C with shaking for 4 hours. Afterward, magnetic beads were added and shaken for 30 minutes. The samples were incubated with Proteinase K (Ambion) at 50°C with shaking for 45 minutes after 5 piles of washing with the wash solution (2×NaCl and sodium citrate, 0.5% SDS, 1×protease inhibitor cocktail), and then heated to 95°C for 10 minutes in a heater. RNA was extracted with TRIzol and analyzed by qRT-PCR (28).

RNA immunoprecipitation

RKO and HCT116 cells (1×10^7 cells/sample) transfected with 3×Flag-tagged AGO2 (6 μg) for 48 hours were lysed in polysome lysis buffer [100 mmol/L KCl, 5 mmol/L $MgCl_2$, 10 mmol/L HEPES, pH 7.0, 0.5% NP-40, 1 mmol/L DTT (dithiothreitol), 100 U/mL RNasin RNase inhibitor, 2 mmol/L vanadyl ribonucleoside complexes solution (Sigma), 25 μL/mL protease inhibitor cocktail]. Anti-Flag antibody (Sigma-Aldrich #F1804, RRID:AB_262044) or control IgG were added to the supernatants and incubated at 4°C overnight. Lysates were then subjected to immunoprecipitation by using M2 agarose (Sigma) followed by washing with polysome lysis buffer four times and polysome lysis buffer plus 1 mol/L urea four times. RNA was released by incubating with 150 μL of polysome lysis buffer with 0.1% SDS and 45 μg proteinase K at 50°C for 30 minutes. Finally, RNA was extracted with a phenol-chloroform-isoamyl alcohol mixture (Sigma) for qRT-PCR analysis.

Chromatin immunoprecipitation assay

Normal RKO and HCT116 cells or cells transfected with siNC or sicircRERE (1×10^7 cells/sample) for 48 hours for chromatin immunoprecipitation (ChIP) were fixed with 1% formaldehyde (Sigma) for 15 minutes at room temperature, followed by washing with PBS twice. After cell collection and lysis, the lysates were sonicated to shear chromatin DNA into 300–500 bp. Supernatants were immunoprecipitated with anti-EP300 antibody (Abcam #ab14984, RRID:AB_301550) or control IgG overnight at 4°C, followed by incubation with protein G magnetic beads (Bio-Rad, 161–4023) for an additional 4 hours. After washing four times, the protein-DNA complex was reversed by heating at 65°C and vortexing at 1,400 rpm for 1 minute every 1 hour overnight using Eppendorf Thermomixer. Finally, immunoprecipitated DNA was purified by QIAquick spin columns (Qiagen).

RNA-FISH

HCT116 and RKO cells plated on cover glass were transfected with siNC or sicircRERE for 48 hours, and fixed with 4% paraformaldehyde (Solarbio) for 10 minutes at room temperature. Then according to the protocol of RiboTM Fluorescent In Situ Hybridization kit (C10910, RiboBio), cells were then permeabilized with 0.5% Triton X-100/PBS for 5 minutes at 4°C and blocked with prehybridization buffer for 30 minutes at 37°C after washing with PBS three times (5 minutes/time). FISH probes labeled with Cy3 of circRERE (40 nmol/L) were added and incubated overnight at 37°C in the dark. Cells were then washed sequentially with hybridization washing buffer I (4×SSC, 0.1%Tween-20), hybridization washing buffer II (2×SSC), and hybridization washing buffer III (1×SSC) at 42°C in the dark. Nuclei were stained with DAPI (0.1 g/mL) and washed three times with PBS. Images were taken by using a Carl Zeiss laser confocal microscope.

Western blotting

Cells were scraped and lysed in lysis buffer containing 100 mmol/L Tris· Cl (pH 6.8), 20% glycerol, 0.02% bromophenol blue, 4% SDS, and 200 mmol/L DTT. Protein lysates were run on a 10% SDS-PAGE gel and transferred onto a polyvinylidene difluoride membrane (Merck Millipore). After blocking with 5% fat-free milk for 1 hour, the membrane was incubated with primary antibodies diluted by 1% fat-free milk [TBK1 (Cell Signaling Technology #38066, RRID:AB_2827657), p-TBK-1 (Cell Signaling Technology #5483, RRID:AB_10693472), p-IRF3 (Cell Signaling Technology #4947, RRID:AB_823547), P65 (Cell Signaling Technology #8242, RRID:AB_10859369), p-P65 (Cell Signaling Technology #3033, RRID:AB_331284), MAVS (Proteintech #14341–1-AP, RRID:AB_10548408), and GAPDH (Protein Tech #60004–1, RRID:AB_2107436) overnight at 4°C and the appropriate secondary antibodies, goat anti-rabbit (Solarbio Cat# SE134, RRID:AB_2797593) or goat anti-mouse (Solarbio # SE131, RRID:AB_2797595), at room temperature for 1 hour. After washing four to six times, the signals were visualized using the ECL detection reagents (K-12045-D50, Advansta).

Subcellular fraction

Subcellular fraction was performed as described previously (29). Cells washed with cold PBS were collected in ice-cold Buffer I (10 mmol/L Hepes, pH 8.0; 1.5 mmol/L $MgCl_2$; 10 mmol/L KCl; 1 mmol/L DTT) to allow cells to swell. After incubation for 15 minutes, NP-40 was added at a final concentration of 1%. Then the supernatants were collected as the cytoplasmic fraction after vortex and centrifugation. Next, the pellet was resuspended with ice-cold Buffer II (20 mmol/L Hepes, pH 8.0; 1.5 mmol/L $MgCl_2$; 25% glycerol; 420 mmol/L NaCl; 0.2 mmol/L EDTA; 1 mmol/L DTT with protease and RNase inhibitors) and rotated vigorously at 4°C for 30 minutes. After centrifuging 15 minutes at maximum speed, the nuclear fraction was collected. Then both cytosolic and nuclear RNAs were extracted for use.

Copy-number analysis

Copy-number analysis was performed following the protocol reported previously (30). Briefly, cells were collected and counted. Serially diluted qRT-PCR products of circRERE and miR-6837–3p were used as templates to formulate standard curves. The exact copy numbers of circRERE and miR-6837–3p per cell were then used and calculated according to the standard curves.

Dual-luciferase reporter assay

The wild-type circRERE [circRERE(WT)] and the wild-type 3′ untranslated region (UTR) of *MAVS* [*MAVS*(WT)] as well as the mutant forms with the potential miR-6837–3p binding sites mutated

[circRERE(MT) and *MAVS*(MT)] were cloned in psiCHECK2 (RRID: Addgene_40763) vector. The promoter sequences from *RERE* gene [*RERE* promoter(WT)] and the mutant form with the EP300 binding site mutated [*RERE* promoter(MT)] were cloned in pGL3-Basic vector. All sequences were listed in Supplementary Table S1.

Cells were seeded into 48-well plates and transfected with luciferase vectors for 48 hours. Luciferase activity was then measured by Spark Multimode Microplate Reader (Tecan) according to the protocol of the Dual-Luciferase Assay System (Promega).

Animal experiments

For experiments to explore the effects of circRERE on tumor growth, RKO cells (1×10^6) stably transfected with control shRNA (shNC) or two individual shRNAs specifically targeting circRERE (shcircRERE-1 and shcircRERE-2) were inoculated subcutaneously in the left inguen of male Balb/c nude mice (5 mice/group; 16–20 g; 6 weeks; Beijing Huafukang Bioscience). All the mice were sacrificed by dislocating the cervical vertebra on the 14th day. To validate the effect of mouse circRere on tumor growth in C57BL/6J mice (IMSR_JAX:000664), MC38 cells stably transfected with control vector or circRere overexpression vector were implanted (5 mice/group) as mentioned above. Mice were sacrificed on the 21st day after implantation.

To test the efficacy of circRERE-AAV treatment on tumor growth, HCT116 (2×10^6) cells suspended in 100 μL of PBS were injected into the left inguen of male Balb/c nude mice (5 mice/group). When the tumors reached approximately 100 mm^3, mice were randomized into two groups. NC-AAV (5×10^8 Pfu/mice) or circRERE-AAV (5×10^8 Pfu/mice) were injected intratumorally once a week. The tumor volume and mice body weight were measured twice a week. Tumor volume was calculated using the following formula: tumor volume (mm^3) = [(length) × (width)^2]/2. Mice were sacrificed on the 14th day after treatment started.

To evaluate the therapeutic effects of combination treatment with circRERE-AAV and anti-PD-1 antibodies, MC38 cells (2×10^6) were inoculated subcutaneously in C57BL/6J mice. Mice were randomly assigned into four groups (5 mice/group) when the tumors reached approximately 100 mm^3. Mice were administrated with NC-AAV or circRere-AAV in the presence or absence of vehicle or anti-PD-1 antibodies (Bio X Cell #BE0146, RRID: AB_10949053). AAV was injected intratumorally once a week, and anti-PD-1 antibodies (200 μg/mouse) were injected intraperitoneally twice a week. The tumor volume and mice body weight were also measured twice a week. Mice were sacrificed on the 14th day after treatment.

The animal experiment was performed in accordance with institutional standard guidelines of Xiamen University (Xiamen, P.R. China) and adhered to the U.S. Public Health Service Policy on the Humane Care and Use of Laboratory Animals.

Immunofluorescence

Tissue specimens were resected, fixed by 4% paraformaldehyde, and embedded in paraffin. A total of 4-μm tissue sections were prepared for staining. After dewaxing and receiving antigen repairing, sections were incubated with primary antibodies against CD8A (Abcam #ab209775, RRID:AB_2860566) or CD3 (Abcam #ab16669, RRID: AB_443425) overnight at 4°C. Then they were incubated with fluorescent secondary antibodies appropriately respond to primary antibody in species for 50 minutes in dark condition and DAPI at room temperature for 10 minutes. After washing with PBS and sealing, the images were obtained by Cellsens Standard software (Olympus).

Data availability statement

All the data supporting the findings of this study are available upon reasonable request. Raw data for RNA-seq were deposited in the Gene Expression Omnibus (RRID:SCR_005012) under accession number GSE224734.

Statistical analysis

For comparison of the two groups in this study, a two-tailed Student *t* test or paired *t* test was conducted. Comparison of multiple comparisons was analyzed by two-way ANOVA. SPSS 20.0 software (RRID: SCR_002865) and GraphPad Prism (RRID:SCR_000306) were used to perform the statistical analysis. Image J (RRID:SCR_003070) was used for colony calculating and WB quantification. $P \leq 0.05$ was considered statistically significant.

Results

circRERE is lowly expressed in colorectal cancer tissues and critical for tumorigenesis

To explore differentially expressed circRNAs in colorectal cancer, three pairs of colorectal cancer and matched adjacent normal tissues were collected for circRNA sequencing (circRNA-seq) analysis. There were 38 and 48 circRNAs upregulated and downregulated in colorectal cancer, respectively ($P < 0.05$, FC > 1.5; **Fig. 1A**). The expression patterns of these dysregulated circRNAs were shown by heatmap (**Fig. 1B**). In this study, we focused on studying circRNAs downregulated in colorectal cancer. Aiming to identify clinically relevant circRNAs, we first determined which parental genes of these circRNAs are clinically relevant based on The Cancer Genome Atlas (TCGA) database, such that they are downregulated in colorectal cancer and predict poor prognosis of patients with colorectal cancer (**Fig. 1C**). The results showed that two genes, RERE and PARM1, are significantly downregulated and predict poor prognosis of colorectal cancer (**Fig. 1D** and **E**; Supplementary Fig. S1A and S1B). We then tested whether circRERE and circPARM1 are required for colorectal cancer cell growth. siRNAs specifically targeting circRERE and circPARM1 junction regions were designed and used for knocking down circRERE and circPARM1, respectively. circRERE, but not circPARM1, was found to be required for the growth of HCT116 cells (Supplementary Fig. S1C and S1D).

The underpresentation of both RERE and circRERE in colorectal cancer tissues was validated by 75 pairs of colorectal cancer and adjacent normal tissues in house (**Fig. 1F**). To explore its function in colorectal cancer cells, we examined the expression levels of circRERE in five different colorectal cancer cell lines (**Fig. 1G**). DLD1 and LoVo were used for overexpression experiments, and HCT116 and RKO were used for knockdown experiments. Overexpression of circRERE inhibited cell proliferation and colony formation in both DLD1 and LoVo cells (**Fig. 1H–K**). Conversely, knockdown of circRERE promoted colorectal cancer cell proliferation and colony formation in both HCT116 and RKO cells (**Fig. 1L–O**). We further examined the effects of circRERE on tumor growth *in vivo*. The weight of tumors derived from MC38 cells stably infected with circRere overexpression vector was dramatically decreased than those stably infected with control vector (**Fig. 1P–R**). In contrast, the weight of tumors derived from HCT116 cells stably infected with shREREs were significantly increased compared with those with shNC (**Fig. 1S** and **T**). Taken together, circRERE is downregulated in colorectal cancer tissues and serves as a tumor suppressor in colorectal cancer.

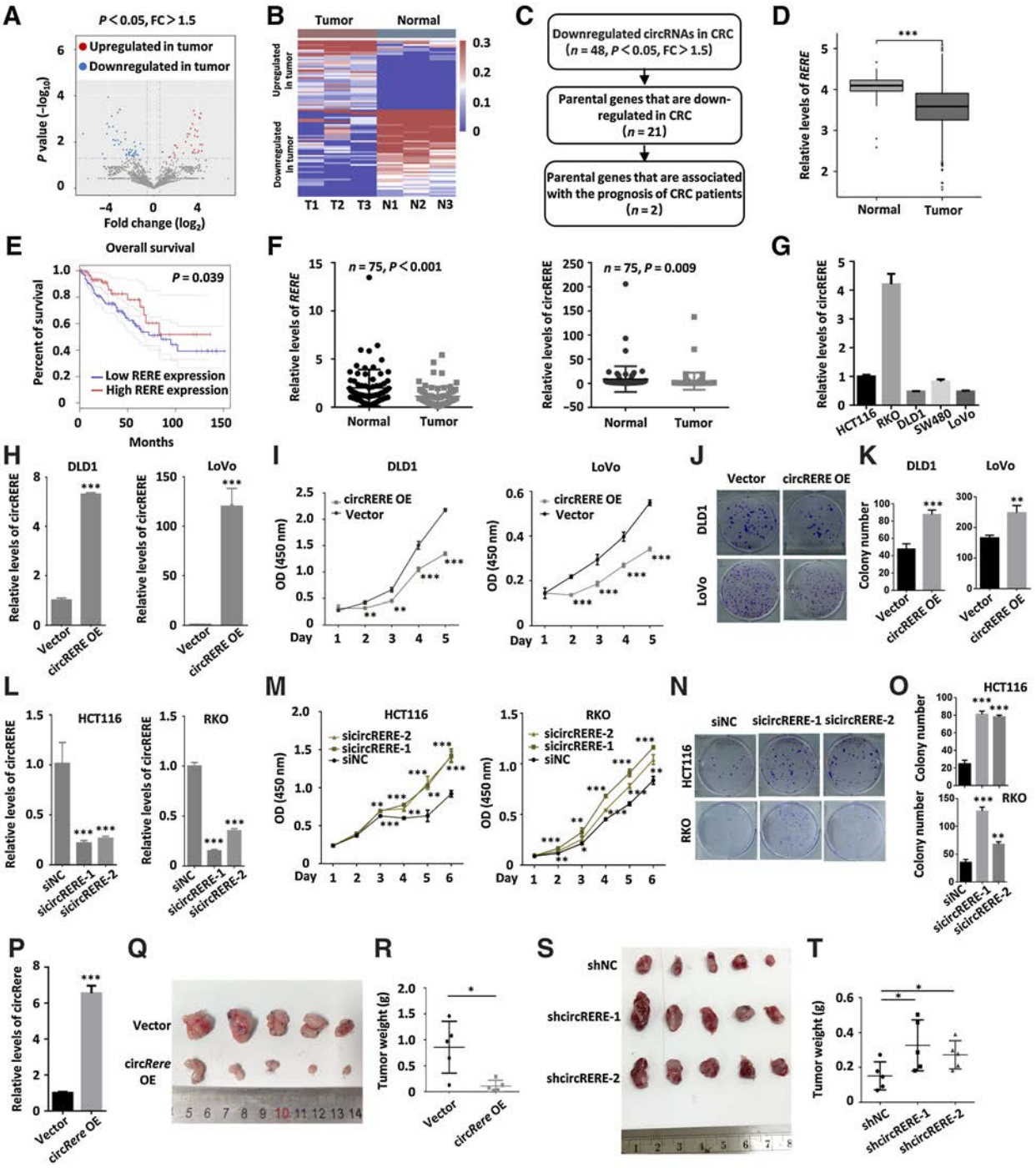

Figure 1.

circRERE is lowly expressed in colorectal cancer tissues and required for colorectal cancer tumorigenesis. **A,** Three pairs of colorectal cancer (T1, T2, T3) and the matched adjacent normal tissues (N1, N2, N3) were subjected to circRNA-seq, and the expression of circRNAs detected is shown by volcano plot. **B,** The expression of the upregulated and downregulated circRNAs in tumors as shown in **A** is shown by heatmap ($P < 0.05$, FC > 1.5). **C,** The flow chart for identifying clinically relevant cirRNAs in colorectal cancer is shown. **D,** The expression of RERE in normal ($n = 41$) and colorectal cancer ($n = 480$) tissues was analyzed on the basis of data from TCGA database. **E,** Kaplan–Meier survival analyses for overall survival of all patients with colorectal cancer using RERE as input is shown. **F,** The expression of RERE (left) and circRERE (right) in 75 pairs of colorectal cancer (T) and the adjacent normal tissues (N) was examined by qRT-PCR analysis. **G,** The expression of circRERE in HCT116, RKO, DLD1, SW480, and LoVo colorectal cancer cell lines was examined by qRT-PCR analysis. **H–J,** DLD1 and LoVo cells infected with control vector or vector expressing circRERE were subjected to qRT-PCR analysis to examine the expression of circRERE (**H**), cell proliferation assay (**I**), and colony formation assay (**J**). (*Continued on the following page.*)

Characteristics of circRERE in colorectal cancer cells

circRERE (has_circ_12952) is generated from exon 3 of gene *RERE*, 469 nucleotides in length. The junction region of circRERE was detectable by divergent primers and confirmed by Sanger sequencing in HCT116 cells (Supplementary Fig. S2A). Then, total RNA extracted from HCT116 cells was digested with RNase R exonuclease and amplified by qRT-PCR. The results showed that circRERE, but not linear RERE, could be amplified after RNase R digestion (Supplementary Fig. S2B). The stability of circRERE and RERE was also tested by treating HCT116 cells with Actinomycin D, an inhibitor of transcription. The result showed that circRERE was much more stable than RERE (Supplementary Fig. S2C).

Next, subcellular localization of circRERE was determined by cellular fraction assay. The results showed that circRERE is mainly localized in the cytoplasm (Supplementary Fig. S2D). RNA-FISH analysis results confirmed the cytosolic localization of circRERE (Supplementary Fig. S2E). Taken together, circRERE is stably localized in the cytoplasm of cells.

circRERE positively regulates the IFNα signaling pathway

We next sought to investigate the underlying mechanisms for circRERE to exert its tumor-suppressive function in colorectal cancer. HCT116 and RKO cell lines transfected with siNC or sicircRERE were collected for RNA-seq. Differential expression analysis results showed that 84 and 84 genes were significantly upregulated and downregulated in both HCT116 and RKO cell lines ($q < 0.05$, FC > 1.2; **Fig. 2A**). The expression of these circRERE-regulated genes was shown by heatmap and box plot (**Fig. 2B** and **C**). Hallmark analysis results revealed that IFNα response was the most enriched for genes positively regulated by circRERE (**Fig. 2D**).

Regulation of *IFNA1* and ISGs such as *ISG15, OAS1, ISG20, IL7, CXCR2, CCR2*, and *CCL5* were confirmed by knockdown and overexpression of circRERE in HCT116 and DLD1 cells, respectively (**Fig. 2E** and **F**). Furthermore, knockdown of circRERE in HCT116 cell-derived xenografts significantly inhibited the expression of IFNA1 and ISGs as listed above, while overexpression of circRere in MC38-derived xenografts significantly induced the expression of these genes (**Fig. 2G** and **H**). And MC38-derived xenografts with circRere overexpression were associated with many more $CD8^+$ T cells than control group (**Fig. 2I**). In summary, circRERE positively regulates the expression of IFNA1 and ISGs, improving antitumor immunity in colorectal cancer.

circRERE acts as a ceRNA to sponge miR-6837-3p to regulate the expression of MAVS and the downstream type I IFN signaling pathway

Type I IFN signaling pathway is mainly modulated by cGAS/STING and RIG-I/MAVS pathways. To investigate the molecular mechanism of how circRERE affects this pathway, we examined the impact of circRERE on the expression of critical regulators in these two pathways including RIG-I, MAVS, cGAS, STING, IFIH1, IRF3, TBK1, IκBα, and DHX58 in HCT116 cells transfected with siNC or sicircREREs. The results showed that only MAVS was significantly decreased upon circRERE knockdown (**Fig. 3A**), which was confirmed in RKO cells (**Fig. 3B**). As expected, circRERE overexpression promoted the expression of MAVS in DLD1 and LoVo cells (**Fig. 3C**). The expression of MAVS and its downstream activation events including the phosphorylation of TBK1, IRF3, and NFκB in response to circRERE knockdown and overexpression were verified by Western blotting (**Fig. 3D** and **E**; Supplementary Fig. S3A and S3B). To test whether circRERE regulated the type I IFN signaling pathway through MAVS, HCT116 cells were infected with circRERE-overexpression vector in the presence or absence of shNC or shMAVS. Knockdown of MAVS significantly attenuated the induction of IFNA1, CXCR2, CCL5, and OASL by circRERE overexpression, suggesting MAVS is required for circRERE-activated IFNα and ISGs (**Fig. 3F** and **G**).

Next, we sought to investigate how circRERE regulates MAVS. circRERE was found to be mainly localized in the cytoplasm, which prompted us to propose that circRERE might act as a miRNA sponge. To this end, RNA immunoprecipitation (RIP) assay with anti-AGO2 antibody was conducted to determine whether circRERE binds to miRNAs. circRERE was successfully pulled down by anti-AGO2 antibody, but not a control IgG, indicating that circRERE might bind with miRNAs (**Fig. 3H** and **I**). Three different algorithms (miRanda, RNAhybrid, and TarPmiR) were then used to predict miRNAs that can bind with circRERE and MAVS. miR-6837–3p was predicted to target both circRERE and the 3′ UTR of MAVS (**Fig. 3J** and **K**). We therefore focused on exploring the ceRNA network including circRERE, miR-6837–3p and MAVS.

To support that circRERE could serve as a miRNA sponge for miR-6837–3p, the copy number of circRERE and miR-6837–3p was comparable in both HCT116 and RKO cells (**Fig. 3L**). To test whether miR-6837–3p can bind to circRERE, chromatin isolation by RNA purification (ChIRP) assay was performed using biotin-labeled control probes or probes specifically targeting circRERE. miR-6837–3p was found to be significantly enriched by circRERE probes, but not control probes (**Fig. 3M**). The linear sequence of circRERE [circRERE(WT)] or its mutant form with the miR-6837–3p binding site mutated [circRERE(MT)] was cloned into a luciferase reporter vector and then transfected with control mimics or miR-6837–3p mimics in HCT116 and RKO cells, followed by luciferase activity measurement (**Fig. 3J** and **N**). Cotransfection of miR-6837–3p mimics significantly reduced the luciferase activity of circRERE(WT), while there was no significant change of circRERE(MT), supporting the binding of miR-6837–3p with circRERE (**Fig. 3N**). Similar experiments were performed to examine the binding of miR-6837–3p with the 3′ UTR of *MAVS*. Cotransfection of miR-6837–3p mimics significantly reduced the luciferase activity of 3′ UTR *MAVS*(WT), but not 3′ UTR *MAVS*(MT), suggesting that miR-6837–3p could also bind to MAVS (**Fig. 3K** and **O**).

We next sought to explore whether the regulation of MAVS by circRERE is through serving as a sponge of miR-6837–3p. To this end,

(*Continued.*) **K,** The quantification of the number of colonies in **J**. **L–N,** HCT116 (left) and RKO (right) cells transfected with control siRNA (siNC) or two individual siRNA specifically targeting circRERE (sicircRERE-1 and sicircRERE-2) were subjected to qRT-PCR analysis to examine the expression of circRERE (**L**), cell proliferation assay (**M**), and colony formation assay (**N**). **O,** The quantification of the number of colonies in **M**. **P,** MC38 cells stably expressing control vector or circRere were subjected to qRT-PCR analysis to examine the expression of circRere. **Q,** MC38 cells stably expressing control vector or circRere were injected into C57BL/6J mice for 3 weeks, and the tumors were collected and photographed. **R,** The weight of tumors as described in **N** is shown. **S,** HCT116 cells stably expressing control shRNA (shNC) or two individual shRNAs targeting circRERE (shcircRERE-1 and shcircRERE-2) were injected into Balb/c nude mice for 2 weeks, and the tumors were collected and photographed. **T,** The weight of tumors as described in **P** is shown. *, $P < 0.05$; **, $P < 0.01$; ***, $P < 0.001$.

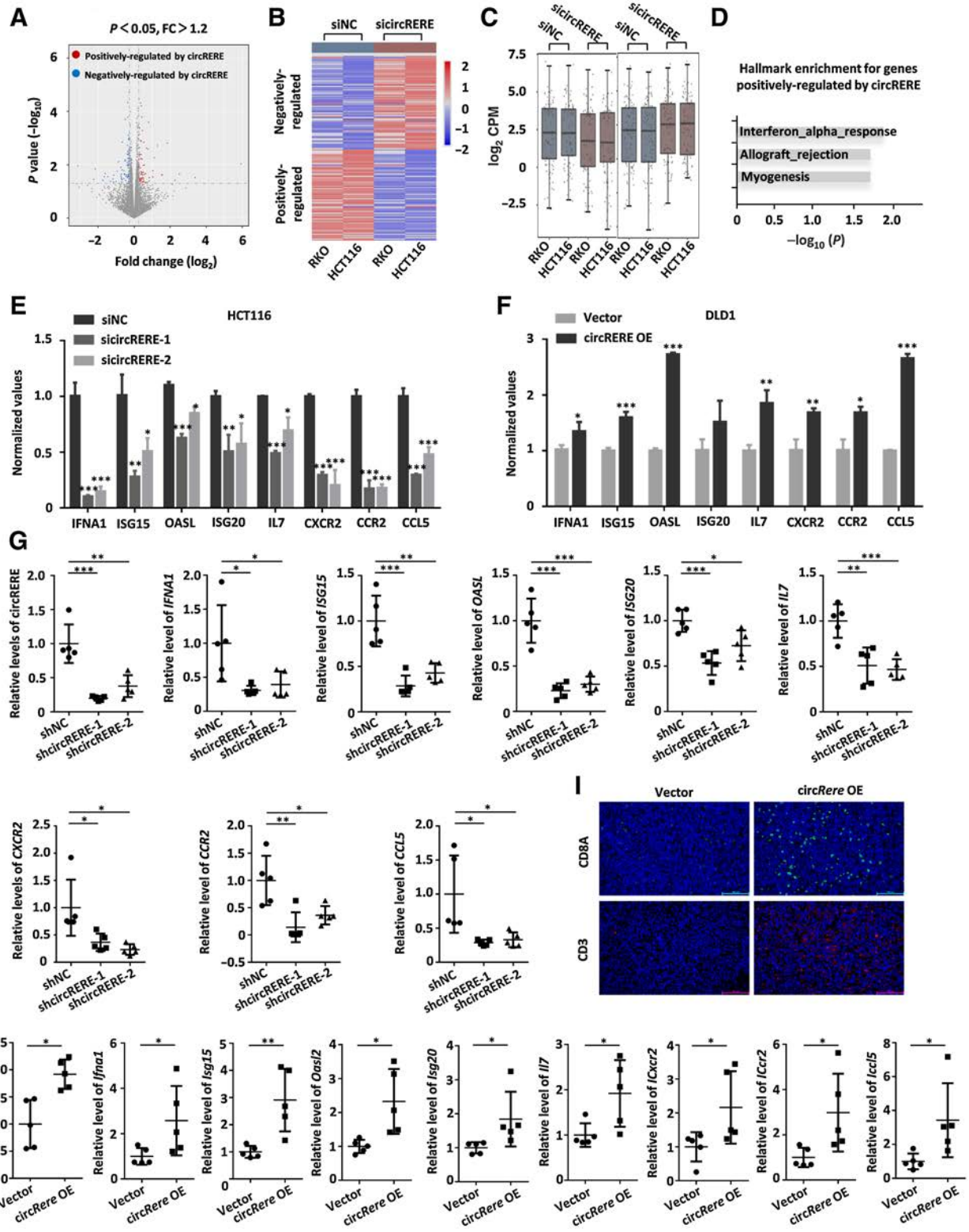

Figure 2.

circRERE positively regulates the type I IFN signaling pathway. **A,** HCT116 and RKO cells transfected with siNC or sicircRERE were subjected to RNA-seq analysis, and the genes positively and negatively regulated by circRERE in both cell lines are shown by volcano plot. **B** and **C,** The expression pattern of genes regulated by circRERE as described in **A** is shown by heatmap (**B**) and box plot (**C**; $q < 0.05$, FC > 1.2). **D,** Hallmark analysis for genes positively regulated by circRERE is shown. **E,** HCT116 cells transfected with siNC or sicircRERE were subjected to qRT-PCR analysis to examine the expression of genes as indicated. **F,** DLD1 cells infected with control vector or vector expressing circRERE (OE) were subjected to qRT-PCR analysis to examine the expression of genes as indicated. **G** and **H,** Tumor samples as shown in **Fig. 1N** (**G**) and **Fig. 1P** (**H**) were subjected to qRT-PCR analysis to examine the expression of genes as indicated. **I,** Tumor sections from **Fig. 1N** were subjected to immunofluorescence staining by anti-CD8A or anti-CD3 specific antibody. *, $P < 0.05$; **, $P < 0.01$; ***, $P < 0.001$.

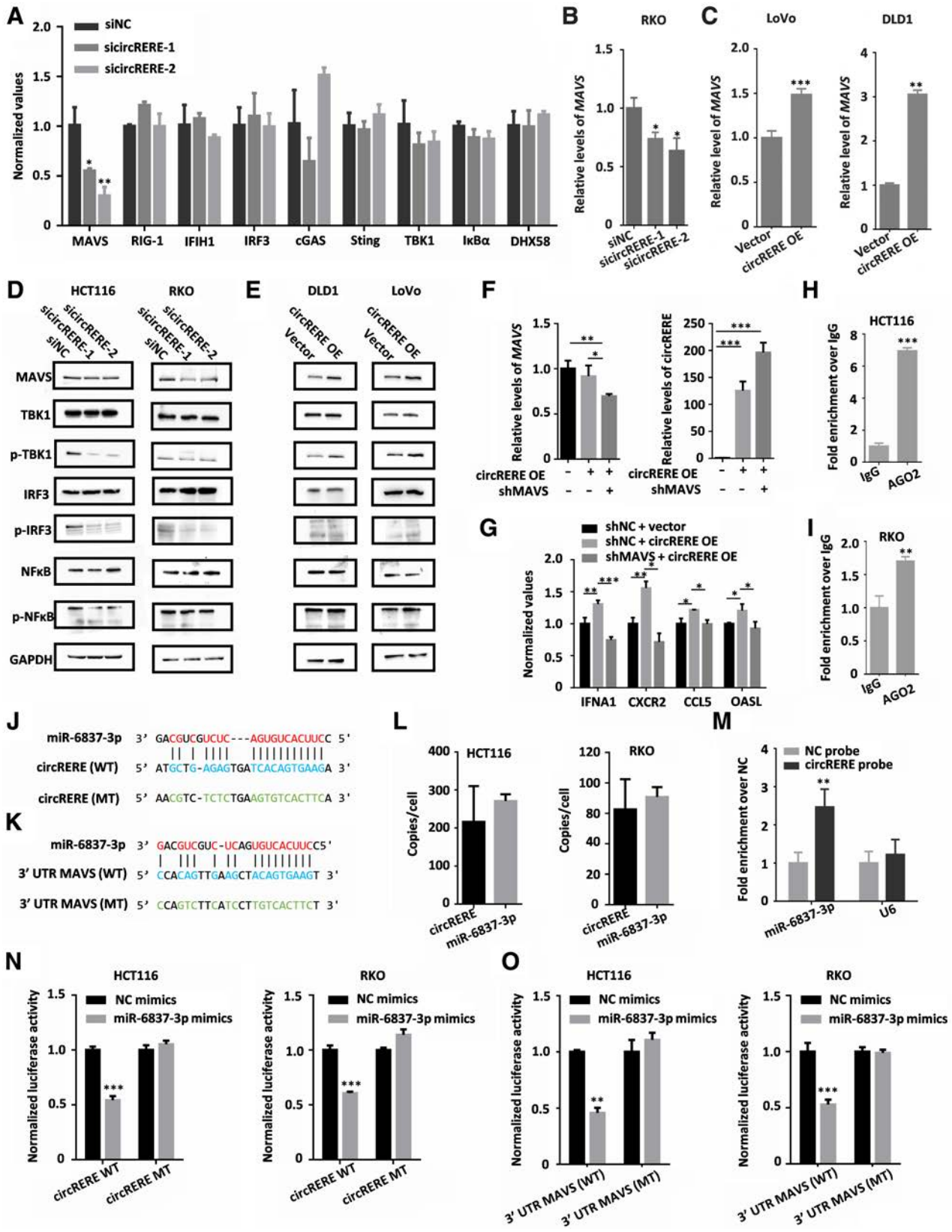
A
siNC
sicircRERE-1
sicircRERE-2
Normalized values
MAVS
RIG-1
IFIH1
IRF3
cGAS
Sting
TBK1
IκBα
DHX58
B
RKO
Relative levels of MAVS
siNC
sicircRERE-1
sicircRERE-2
C
LoVo
DLD1
Relative level of MAVS
Vector
circRERE OE
D
HCT116
RKO
MAVS
TBK1
p-TBK1
IRF3
p-IRF3
NFκB
p-NFκB
GAPDH
E
DLD1
LoVo
F
Relative levels of MAVS
Relative levels of circRERE
circRERE OE
shMAVS
H
HCT116
Fold enrichment over IgG
IgG
AGO2
G
shNC + vector
shNC + circRERE OE
shMAVS + circRERE OE
Normalized values
IFNA1
CXCR2
CCL5
OASL
I
RKO
J
miR-6837-3p 3' GACGUCGUCUC---AGUGUCACUUCC 5'
circRERE (WT) 5' ATGCTG-AGAGTGATCACAGTGAAGA 3'
circRERE (MT) 5' AACGTC-TCTCTGAAGTGTCACTTCA 3'
K
miR-6837-3p 3' GACGUCGUC-UCAGUGUCACUUCC5'
3' UTR MAVS (WT) 5' CCACAGTTGAAGCTACAGTGAAGT 3'
3' UTR MAVS (MT) 5' CCAGTCTTCATCCTTGTCACTTCT 3'
L
HCT116
RKO
Copies/cell
circRERE
miR-6837-3p
M
NC probe
circRERE probe
Fold enrichment over NC
miR-6837-3p
U6
N
HCT116
RKO
NC mimics
miR-6837-3p mimics
Normalized luciferase activity
circRERE WT
circRERE MT
O
HCT116
RKO
NC mimics
miR-6837-3p mimics
Normalized luciferase activity
3' UTR MAVS (WT)
3' UTR MAVS (MT)

HCT116 and RKO cells were transfected with siNC or sicircREREs in the presence or absence of miR-6837–3p inhibitor. As expected, knockdown of circRERE resulted in a decrease in MAVS expression at both protein and mRNA levels, and miR-6837–3p inhibitor cotransfection rescued the decrease in MAVS, indicating that the regulation of MAVS by circRERE was dependent on miR-6837–3p (**Fig. 4A–C**). Consistently, downstream target genes such as *IFNA1, ISG15, OASL*, and *CXCR2* were also significantly recovered by miR-6837–3p inhibitors cotransfection (**Fig. 4D** and **E**). Finally, we tested whether miR-6837–3p is involved in circRERE-regulated colorectal cancer cell growth. miR-6837–3p was found to promote cell proliferation in colorectal cancer cells (Supplementary Fig. S4A and S4B). Furthermore, miR-6837–3p was required for circRERE-regulated colorectal cancer cell growth (**Fig. 4F–H**). Taken together, circRERE activates the type I IFN signaling pathway and inhibits colorectal cancer cell growth by stabilizing MAVS expression through sponging miR-6837–3p.

circRERE is regulated by EP300 in colorectal cancer

The tumor-suppressive role of circRERE in colorectal cancer prompted us to further examine the molecular mechanisms underlying its low expression. In light of the fact that circRERE is transcribed from *RERE*, we hypothesized that transcription factors involved in *RERE* transcription could have a similar impact on circRERE. First, we predicted transcription factors binding to the *RERE* promoter region through PROMO database. It was found that 40 transcription factors have the potential (Supplementary Fig. S5A). The expression of these 40 transcription factors in colorectal cancer tissues was then analyzed based on data from TCGA database. Nine transcription factors including CEBPA, DBP, EP300, ETS1, GATA1, HOXD10, STAT4, TCF4, and VDR are lowly expressed in colorectal cancer tissues compared with the matched adjacent normal tissues (**Fig. 5A**; Supplementary Fig. S5B). In addition, the correlation between the expression of RERE and the above nine transcription factors was analyzed, revealing that EP300 is most correlated with RERE (**Fig. 5B**; Supplementary Fig. S5C).

To determine whether EP300 regulates circRERE, we performed qRT-PCR analysis and showed knockdown of EP300 led to decrease of circRERE, whereas activation of EP300 by using the dCas9-VP64 system exhibited the opposite effects in both HCT116 and RKO cells (**Fig. 5C–F**). We then examined EP300 binding with *RERE* promoter region through ChIP analysis, revealing that EP300, but not a control IgG, was enriched on the two regions in RERE promoter predicted to have EP300 binding (**Fig. 5G**). Knockdown of EP300 significantly attenuated EP300 binding on *RERE* promoter region, strengthening the specificity of the binding detected (**Fig. 5H**). To further verify EP300 binding with *RERE* promoter, *RERE* promoter sequence [*RERE* promoter(WT)] or the mutant form with the EP300 binding sites mutated [*RERE* promoter(MT)] was cloned into a luciferase reporter vector. Cotransfection of EP300 significantly increased the luciferase activity of *RERE* promoter(WT), but not *RERE* promoter(MT) (**Fig. 5I**). Our data therefore suggested EP300 regulated the expression of circRERE by binding to the *RERE* promoter.

We next tested whether EP300 affects MAVS expression. Knockdown of EP300 reduced MAVS expression, while overexpression of EP300 exhibited the opposite effects in both HCT116 and RKO cells (**Fig. 5J–M**; Supplementary Fig. S3C and S3D). To further test whether EP300 regulates the expression of MAVS through circRERE, HCT116 cells with EP300 overexpression were infected with shNC or shcircRERE. EP300 overexpression led to a significant increase in MAVS at both mRNA and protein levels, which was largely abolished when circRERE was knocked down, suggesting EP300 regulates MAVS expression through circRERE (**Fig. 5N–O**; Supplementary Fig. S3E). Taken together, EP300 plays a positive role in regulating the expression of cirRERE and hence MAVS in colorectal cancer.

cirRERE-AAV is potent in inhibiting colorectal cancer tumor growth and capable of improving the therapeutic effects of anti-PD-1 antibody

The tumor-suppressive role of circRERE prompted us to explore whether circRERE can serve as a therapeutic target in colorectal cancer. To this end, mice were inoculated subcutaneously with HCT116 cells, and then were randomly assigned into two groups and treated with NC-AAV or circRERE-AAV once a week. As compared with the NC-AAV, tumors treated with circRERE-AAV were markedly reduced (**Fig. 6A–C**). The body weight of mice from both groups had no significant difference (**Fig. 6D**). To link circRERE-regulated target genes to its function in tumor growth, tumors treated with circRERE-AAV expressed significantly higher levels of circRERE, MAVS, IFNA1, and ISGs (**Fig. 6E**).

MAVS-mediated type I IFN signaling pathway has been well suggested to enhance antitumor immunity by recruiting immune cells such as T cells. It is therefore possible that circRERE-AAV would increase the effectiveness of ICIs such as anti-PD-1 antibody. Mice were subcutaneously inoculated with MC38 cells, and then randomly assigned into four groups and treated with NC-AAV or circRere-AAV in the presence or absence of anti-PD-1 antibody for 2 weeks. Combination treatment with circRere-AAV and

Figure 3.

circRERE acts as a ceRNA to sponge miR-6837-3p to regulate the expression of MAVS. **A** and **B,** HCT116 (**A**) or RKO (**B**) cells transfected with siNC or sicircRERE were subjected to qRT-PCR analysis to examine the expression of genes as indicated. **C,** DLD1 (left) and LoVo (right) cells infected with control vector or vector expressing circRERE (OE) were subjected to qRT-PCR analysis to examine the expression of genes as indicated. **D,** HCT116 (left) or RKO (right) cells transfected with siNC or sicircRERE were subjected to immunoblotting analysis using antibodies as indicated. **E,** DLD1 (left) and LoVo (right) cells infected with control vector or vector expressing circRERE (OE) were subjected to immunoblotting analysis using antibodies as indicated. **F** and **G,** HCT116 cells overexpressed with circRERE were infected with control shRNA (shNC) or shRNA specifically targeting MAVS (shMAVS), followed by qRT-PCR to examine the expression of genes as indicated. **H** and **I,** HCT116 (**H**) or RKO (**I**) cells were subjected to RIP assay using control IgG or anti-AGO2 antibody, followed by qRT-PCR to detect circRERE enrichment. **J** and **K,** The sequence match between miR-6837-3p and the linear sequence of circRERE [circRERE (WT)] (**J**) and the 3′ UTR of *MAVS* [3′ UTR *MAVS* (WT)] (**K**) as well as the mutant form with the potential miR-6837-3p binding site mutated [circRERE (MT) or 3′ UTR *MAVS* (MT)]. **L,** The copy number of circRERE and miR-6837-3p in HCT116 (left) and RKO (right) cells is shown. **M,** HCT116 cells were subjected to ChIRP assay using biotin-labeled control probe or probe specifically targeting circRERE, followed by qRT-PCR analysis to detect the enrichment of miR-6837-3p and U6 snRNA. **N** and **O,** circRERE (WT), circRERE (MT), 3′ UTR *MAVS* (WT), and 3′ UTR *MAVS* (MT) sequences were cloned into psiCHECK2 vectors, which were then transfected into HCT116 and RKO cells with control or miR-6837-3p mimics, followed by luciferase activity measurement. *, $P < 0.05$; **, $P < 0.01$; ***, $P < 0.001$.

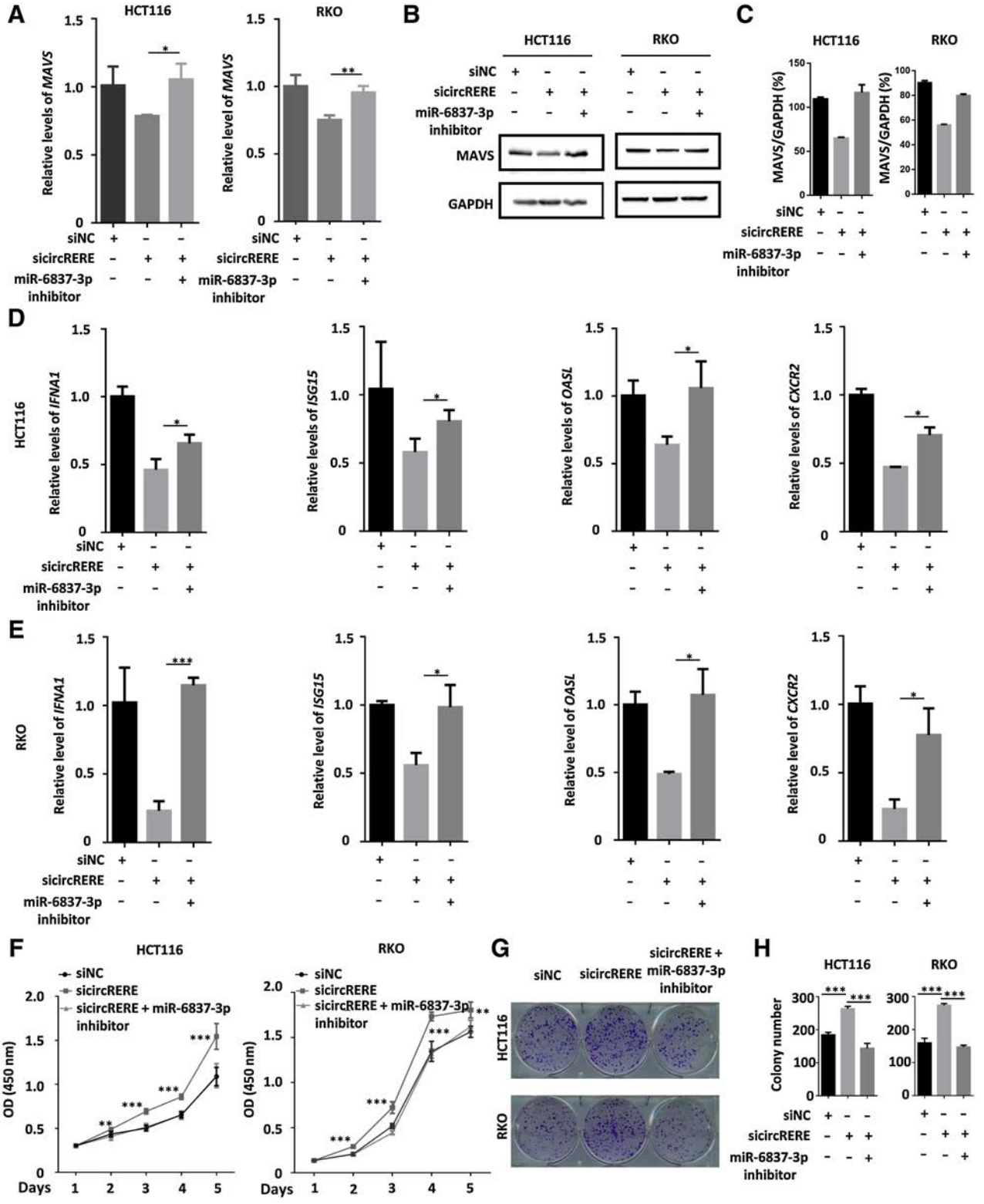

Figure 4.

The regulation of MAVS by circRERE is dependent on miR-6837–3p. **A** and **B,** HCT116 and RKO cells transfected with siNC or sicircRERE in the presence or absence of miR-6837-3p inhibitors were subjected to qRT-PCR (**A**) or immunoblotting (**B**) analysis to examine the expression of MAVS. **C,** The representative densitometry graphic of **B**. **D**–**G,** HCT116 and RKO cells as described in **A** and **B** were subjected to qRT-PCR analysis to determine the expression of genes as indicated (**D** and **E**), cell proliferation assay (**F**), and colony formation assay (**G**). **H,** The quantification of the number of colonies in **G**. *, $P < 0.05$; **, $P < 0.01$; ***, $P < 0.001$.

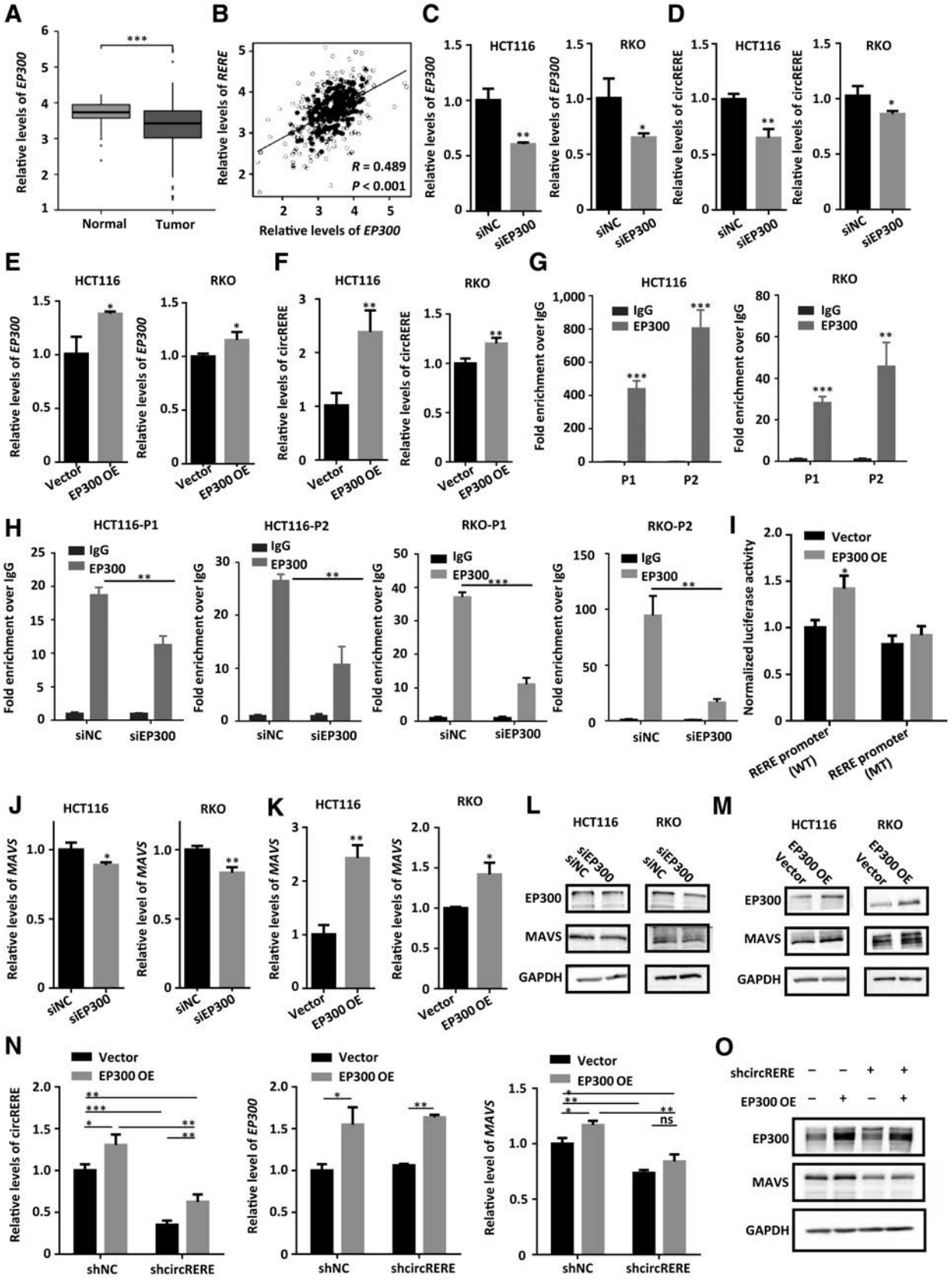
A
Relative levels of EP300
***
Normal
Tumor
B
Relative levels of RERE
R = 0.489
P < 0.001
Relative levels of EP300
C
HCT116
RKO
Relative levels of EP300
siNC
siEP300
D
HCT116
RKO
Relative levels of circRERE
siNC
siEP300
E
HCT116
RKO
Relative levels of EP300
Vector
EP300 OE
F
HCT116
RKO
Relative levels of circRERE
Vector
EP300 OE
G
HCT116
RKO
IgG
EP300
Fold enrichment over IgG
P1
P2
H
HCT116-P1
HCT116-P2
RKO-P1
RKO-P2
IgG
EP300
Fold enrichment over IgG
siNC
siEP300
I
Vector
EP300 OE
Normalized luciferase activity
RERE promoter (WT)
RERE promoter (MT)
J
HCT116
RKO
Relative levels of MAVS
siNC
siEP300
K
HCT116
RKO
Relative levels of MAVS
Vector
EP300 OE
L
HCT116
RKO
siNC
siEP300
EP300
MAVS
GAPDH
M
HCT116
RKO
Vector
EP300 OE
EP300
MAVS
GAPDH
N
Vector
EP300 OE
Relative levels of circRERE
Relative level of EP300
Relative level of MAVS
ns
shNC
shcircRERE
O
shcircRERE
EP300 OE
EP300
MAVS
GAPDH

anti-PD-1 antibody led to a markedly decreased tumor weight compared with control group or groups treated with circRere-AAV or anti-PD-1 alone (**Fig. 6F**-**H**). The body weight of all mice did not show any significant changes (**Fig. 6I**). Combination treatment with circRere-AAV and ani-PD-1 antibody resulted in the most dramatic increase of $CD8^+$ and $CD3^+$ T-cell infiltration compared with other groups (**Fig. 6J**). Taken together, circRERE-AAV is potent in inhibiting tumor growth, and capable of improving the therapeutic effects of anti-PD-1 antibodies in colorectal cancer.

Discussion

Over the past few years, immunotherapy is considered an innovation and has become a trend in the field of tumor treatment (31). The most popular immunotherapy is ICIs, which relieve the immune system from suppression by tumor cells and restart immune responses. However, clinical studies have shown that ICIs only work in a small portion of patients with microsatellite instability. For patients with low-grade microsatellite instability, immunotherapy has limited effects. These tumors are what we call "cold tumors," responding extremely poorly to immunotherapy (32, 33). It is important to note that the proportion of patients with microsatellite instability is only 5% of total, and the incidence gradually decreases with increasing tumor stage. Searching for therapeutic targets to improve immunotherapy responses among patients with colorectal cancer is of great clinical significance. Multiple studies have indicated that circRNAs play a key role in immune regulation and immunotherapy (12–15). These circRNAs are involved in almost all key processes of antitumor immunity and are potential biomarkers and therapeutic targets for immunotherapy. However, the mechanism underlying circRNAs regulation of immune responses is largely unknown and should be further elucidated to help patients' better benefit from immunotherapy.

In this study, we found that circRERE, a lowly expressed circRNA in colorectal cancer, acted as a tumor suppressor. Transcriptomics analysis highlighted type I IFN signaling pathway as the major circRERE-regulated downstream target gene program. Activation of type I IFN signaling has both direct and indirect antitumor effects (34). The direct antitumor effects are achieved through apoptosis, cell-cycle arrest, and antiangiogenic activity (35–37). The indirect antitumor effects are mainly through immune regulation. It has been shown that the production of IFNs and other proinflammatory cytokines can activate $CD4^+$ Th cells, $CD8^+$ cytotoxic T cells, NK cells, dendritic cells, and macrophages to participate in the immune response to tumors (38–41). The activation of RIG-I/MAVS can promote the phosphorylation of IRF3/7 and NFκB, thus inducing type I IFN and other proinflammatory cytokines. MAVS is an essential adaptor protein that induces type I IFN signaling. Its expression, both post-transcriptionally and posttranslationally, is regulated by multiple mechanisms (42, 43). Our study indicated that circRERE could compete with MAVS for binding with miR-6837–3p, thus stabilizing MAVS and promoting MAVS-mediated downstream phosphorylation of TBK1, IRF3, and P65. Further rescue assays confirmed that the regulation of MAVS by circRERE was dependent on miR-6837–3p.

Because circRERE plays an important role in cancer, it is of great importance to examine how circRERE is regulated in colorectal cancer. By bioinformatics prediction and experimental validation, we found EP300 could bind to the promoter of *RERE* and promote the transcription of circRERE. EP300 functions as a histone acetyltransferase that regulates transcription through chromatin remodeling and plays an essential role in cell proliferation and differentiation. Data from TCGA database showed EP300 was lowly expressed in colorectal cancer tissues and highly correlated with RERE expression. EP300 inhibition of MAVS expression was dependent on circRERE. Therefore, the modulatory axis of EP300/circRERE/miR-6837–3p/MAVS/type I IFN pathway was established to regulate tumor immunity in colorectal cancer (Supplementary Fig. S6).

Compared with linear RNAs, circRNAs are more resistant to exonucleases and are considered one of the most promising candidates for RNA therapy (44). AAV vector is one of the most widely used gene therapy viral vectors. To explore whether circRERE can be a target for colorectal cancer intervention, we successfully constructed an AAV vector that could express circRERE, and demonstrated that intratumoral injection circRERE was potent in inhibiting tumor growth. Activation of pattern recognition receptors such as RIG-1 results in downstream activation of proinflammatory genes, which can elicit a cascade to recruit and activate immune cells that are critical for the initiation of an antitumor immune response (45). Priming the immune response is a potential method for sensitizing the effect of ICIs. Cotreatment of circRERE-AAV and anti-PD-1 antibody recruited more $CD8^+$ T cells to the tumor microenvironment. circRERE-AAV could significantly increase the antitumor effects of anti-PD-1 antibody in colorectal cancer.

In conclusion, we found that circRERE, a EP300-regulated and cytoplasmic-localized circRNA, was lowly expressed in colorectal cancer and functioned as a tumor suppressor. circRERE induced type I IFN signaling pathway to participate in the immune responses by increasing MAVS expression through sponging miR-6837–3p. circRERE-AAV elicited potent antitumor efficacy in colorectal cancer preclinical models and enhanced the antitumor effects of anti-PD-1 antibody. Targeting circRERE might represent a new avenue for

Figure 5.

EP300 regulates the expression of circRERE. **A,** The expression of EP300 in normal ($n = 41$) and colorectal cancer ($n = 480$) tissues was analyzed on the basis of the data from TCGA database. **B,** The correlation between the expression of EP300 and RERE in colorectal cancer tissues ($n = 480$) was analyzed based on the data from TCGA database. **C** and **D,** HCT116 and RKO cells transfected with control siRNA (siNC) or siRNA specifically targeting EP300 (siEP300) were subjected to RNA extraction and qRT-PCR analysis to examine the expression of EP300 (**C**) and circRERE (**D**). **E** and **F,** HCT116 and RKO cells infected with lentivirus expressing control sgRNA or sgRNA targeting *EP300* gene promoter fused to dCas9-VP64 transcriptional activator were subjected to RNA extraction and qRT-PCR analysis to examine the expression of EP300 (**E**) and circRERE (**F**). **G,** HCT116 and RKO cells were subjected to ChIP analysis with control IgG or anti-EP300 antibody, followed by qRT-PCR analysis using two primer sets (P1 and P2) targeting the two EP300 binding sites predicted in the *RERE* promoter region. **H,** HCT116 and RKO cells were transfected with siNC or siEP300 followed by ChIP-qPCR analysis as described in **G**. **I,** The *RERE* promoter sequence [*RERE* promoter (WT)] and the mutant form with the predicted EP300 binding sites mutated [*RERE* promoter (MT)] were cloned into pGL3-basic luciferase reporter vector, which were then transfected into HEK293T cells in the presence or absence of control vector or vector expressing EP300, followed by luciferase activity measurement. **J** and **L,** HCT116 and RKO cells as described in **C** and **D** were subjected to qRT-PCR (**J**) analysis and immunoblotting analysis (**L**) as indicated to examine the expression of MAVS. **K** and **M,** HCT116 and RKO cells as described in **E** and **F** were subjected to qRT-PCR (**K**) analysis and immunoblotting analysis (**M**) to examine the expression of MAVS. **N,** HCT116 cells stably expressing shNC or shcircRERE were infected with lentivirus expressing control sgRNA or sgRNA targeting *EP300* gene promoter fused to dCas9-VP64 transcriptional activator, followed by RNA extraction and qRT-PCR analysis to examine the expression of circRERE, EP300, and MAVS. **O,** HCT116 cells as described in **N** were subjected to immunoblotting analysis using antibodies as indicated. *, $P < 0.05$; **, $P < 0.01$; ***, $P < 0.001$.

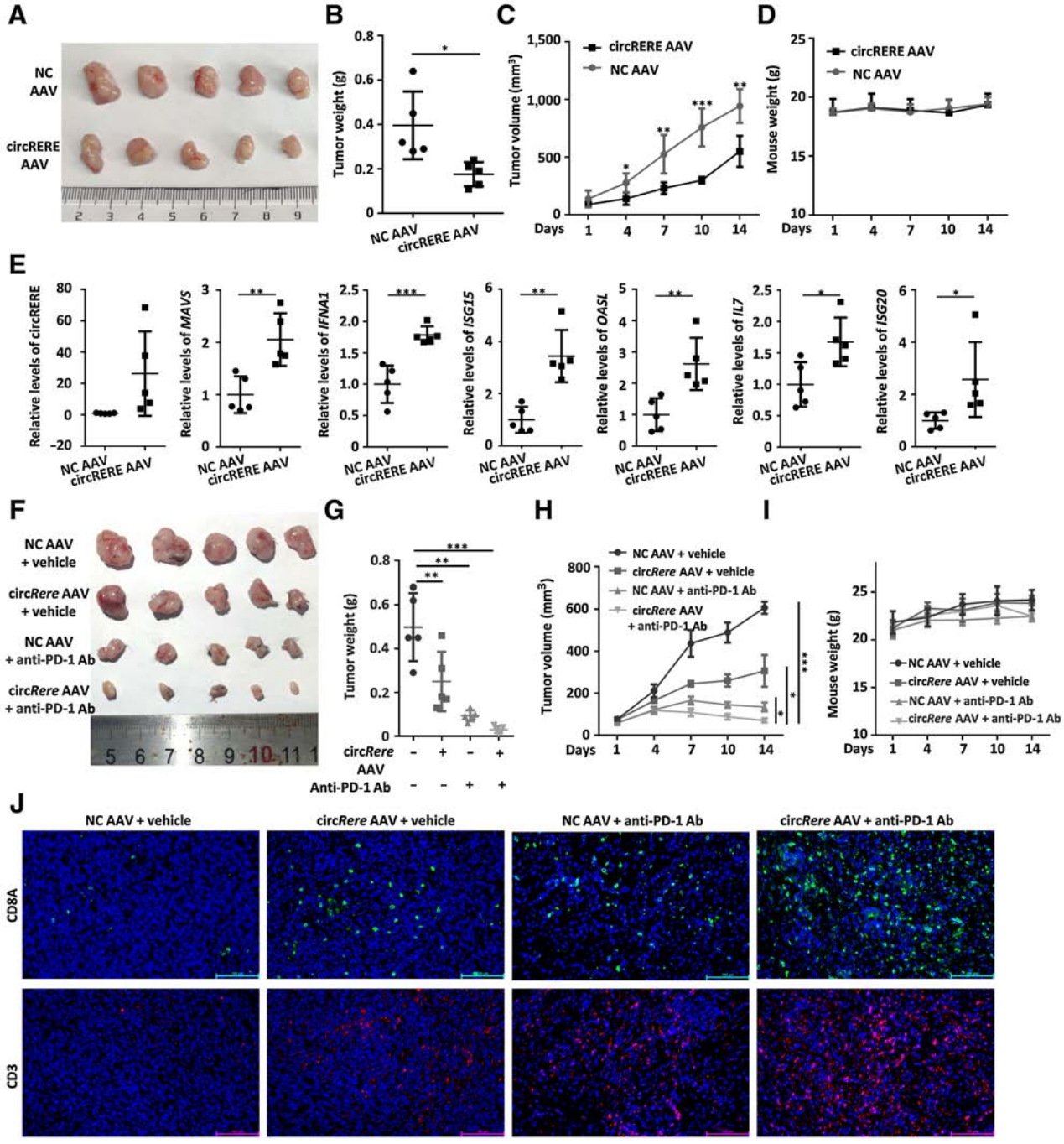

Figure 6.

circRERE-AAV is potent in inhibiting colorectal cancer tumor growth and capable of improving the therapeutic effects of anti-PD-1 antibodies. **A,** Balb/c nude mice were subcutaneously implanted with HCT116 cells, and treated with AAV-expressing negative control vector (NC-AAV) or circRERE (circRERE-AAV) for 2 weeks (once per week), and the tumors were collected and photographed. **B,** The weight of tumors as described in **A** is shown. **C,** The growth curve of tumors as described in **A** is shown. **D,** The body weight of mice as described in **A** is shown. **E,** The tumors as described in **A** were subjected to RNA extraction and qRT-PCR analysis to detect the expression of genes as indicated. **F,** C57BL/6J mice were subcutaneously implanted with MC38 cells, and treated with NC-AAV or circRere-AAV (once per week) in the presence or absence of anti-PD-L1 antibody for 2 weeks (twice per week), and the tumors were collected and photographed. **G,** The weight of tumors as described in **F** is shown. **H,** The growth curve of tumors as described in **F** is shown. **I,** The body weight of mice as described in **F** is shown. **J,** Tumor sections from **F** were subjected to immunofluorescence staining by anti-CD8A or anti-CD3 specific antibodies. *, $P < 0.05$; **, $P < 0.01$; ***, $P < 0.001$.

priming the immune system and enhancing the therapeutic effects of immunotherapy in colorectal cancer in clinic.

Authors' Disclosures

No disclosures were reported.

Authors' Contributions

N. Ding: Conceptualization, data curation, funding acquisition, investigation, writing–original draft, project administration. **A.-B. You:** Conceptualization, formal analysis, validation, methodology, writing–original draft, project administration. **H. Yang:** Formal analysis, investigation. **G.-S. Hu:** Software, formal analysis. **C.-P. Lai:** Formal analysis, investigation. **W. Liu:** Conceptualization, resources, supervision, funding acquisition, writing–review and editing. **F. Ye:** Conceptualization, resources, supervision, writing–review and editing.

Acknowledgments

This work was supported by the National Key Research and Development Program of China (2020YFA0112300 and 2020YFA0803600), National Natural Science Foundation of China (82125028, 91953114, 31871319, 81761128015, and 81861130370), Natural Science Foundation of Fujian Province of China (2020J02004), and the Fundamental Research Funds for the Central University (20720190145 and 20720220003) to W. Liu, start-up funds for the introduction of talents from the First Affiliated Hospital of Xiamen University (3502Z20214ZD3010), Health Youth Scientific Research Project of Fujian Province (2020QNB057), and the Natural Science Foundation of Fujian Province, China (2022J05304) to N. Ding, and Health Youth Scientific Research Project of Fujian Province (2021QNB015) and the Natural Science Foundation of Fujian Province, China (2021J05291) to A.-B. You, and the Natural Science Foundation of Fujian Province, China (2020J011238) to F. Ye.

The publication costs of this article were defrayed in part by the payment of publication fees. Therefore, and solely to indicate this fact, this article is hereby marked "advertisement" in accordance with 18 USC section 1734.

Note

Supplementary data for this article are available at Clinical Cancer Research Online (http://clincancerres.aacrjournals.org/).

Received December 14, 2022; revised February 15, 2023; accepted March 21, 2023; published first March 23, 2023.

References

1. Sung H, Ferlay J, Siegel RL, Laversanne M, Soerjomataram I, Jemal A, et al. Global Cancer Statistics 2020: GLOBOCAN estimates of incidence and mortality worldwide for 36 cancers in 185 countries. CA Cancer J Clin 2021;71:209–49.
2. Hansen TB, Jensen TI, Clausen BH, Bramsen JB, Finsen B, Damgaard CK, et al. Natural RNA circles function as efficient microRNA sponges. Nature 2013;495:384–8.
3. Kristensen LS, Andersen MS, Stagsted LVW, Ebbesen KK, Hansen TB, Kjems J. The biogenesis, biology and characterization of circular RNAs. Nat Rev Genet 2019;20:675–91.
4. Zheng Q, Bao C, Guo W, Li S, Chen J, Chen B, et al. Circular RNA profiling reveals an abundant circHIPK3 that regulates cell growth by sponging multiple miRNAs. Nat Commun 2016;7:11215.
5. Dudekula DB, Panda AC, Grammatikakis I, De S, Abdelmohsen K, Gorospe M. CircInteractome: a web tool for exploring circular RNAs and their interacting proteins and microRNAs. RNA Biol 2016;13:34–42.
6. Ashwal-Fluss R, Meyer M, Pamudurti NR, Ivanov A, Bartok O, Hanan M, et al. circRNA biogenesis competes with pre-mRNA splicing. Mol Cell 2014;56:55–66.
7. Legnini I, Di Timoteo G, Rossi F, Morlando M, Briganti F, Sthandier O, et al. Circ-ZNF609 is a circular RNA that can be translated and functions in myogenesis. Mol Cell 2017;66:22–37.
8. Yang Y, Gao X, Zhang M, Yan S, Sun C, Xiao F, et al. Novel role of FBXW7 circular RNA in repressing glioma tumorigenesis. J Natl Cancer Inst 2018;110:304–15.
9. Shang A, Gu C, Wang W, Wang X, Sun J, Zeng B, et al. Exosomal circPACRGL promotes progression of colorectal cancer via the miR-142–3p/miR-506–3p-TGF-β1 axis. Mol Cancer 2020;19:117.
10. Han K, Wang FW, Cao CH, Ling H, Chen JW, Chen RX, et al. CircLONP2 enhances colorectal carcinoma invasion and metastasis through modulating the maturation and exosomal dissemination of microRNA-17. Mol Cancer 2020;19:60.
11. Zhang X, Yao J, Shi H, Gao B, Zhou H, Zhang Y, et al. Hsa_circ_0026628 promotes the development of colorectal cancer by targeting SP1 to activate the Wnt/β-catenin pathway. Cell Death Dis 2021;12:802.
12. Zhang XL, Xu LL, Wang F. Hsa_circ_0020397 regulates colorectal cancer cell viability, apoptosis and invasion by promoting the expression of the miR-138 targets TERT and PD-L1. Cell Biol Int 2017;41:1056–64.
13. Ou ZL, Luo Z, Wei W, Liang S, Gao TL, Lu YB. Hypoxia-induced shedding of MICA and HIF1A-mediated immune escape of pancreatic cancer cells from NK cells: role of circ_0000977/miR-153 axis. RNA Biol 2019;16:1592–603.
14. Ma Y, Zhang C, Zhang B, Yu H, Yu Q. circRNA of AR-suppressed PABPC1 91 bp enhances the cytotoxicity of natural killer cells against hepatocellular carcinoma via upregulating UL16 binding protein 1. Oncol Lett 2019;17:388–97.
15. Li B, Zhu L, Lu C, Wang C, Wang H, Jin H, et al. circNDUFB2 inhibits non-small cell lung cancer progression via destabilizing IGF2BPs and activating anti-tumor immunity. Nat Commun 2021;12:295.
16. Zhang Q, Wang W, Zhou Q, Chen C, Yuan W, Liu J, et al. Roles of circRNAs in the tumour microenvironment. Mol Cancer 2020;19:14.
17. Reikine S, Nguyen JB, Modis Y. Pattern recognition and signaling mechanisms of RIG-I and MDA5. Front Immunol 2014;5:342.
18. Wu B, Hur S. How RIG-I like receptors activate MAVS. Curr Opin Virol 2015;12:91–8.
19. Loo YM, Gale M Jr. Immune signaling by RIG-I-like receptors. Immunity 2011;34:680–92.
20. Chen Q, Sun L, Chen ZJ. Regulation and function of the cGAS-STING pathway of cytosolic DNA sensing. Nat Immunol 2016;17:1142–9.
21. Kolakofsky D, Kowalinski E, Cusack S. A structure-based model of RIG-I activation. RNA 2012;18:2118–27.
22. González-Navajas JM, Lee J, David M, Raz E. Immunomodulatory functions of type I interferons. Nat Rev Immunol 2012;12:125–35.
23. De Maeyer E, De Maeyer-Guignard J. Type I interferons. Int Rev Immunol 1998;17:53–73.
24. Wang L, Yi J, Lu LY, Zhang YY, Wang L, Hu GS, et al. Estrogen-induced circRNA, circPGR, functions as a ceRNA to promote estrogen receptor-positive breast cancer cell growth by regulating cell cycle-related genes. Theranostics 2021;11:1732–52.
25. Betel D, Wilson M, Gabow A, Marks DS, Sander C. The microRNA.org resource: targets and expression. Nucleic Acids Res 2008;36:D149–153.
26. Rehmsmeier M, Steffen P, Hochsmann M, Giegerich R. Fast and effective prediction of microRNA/target duplexes. RNA 2004;10:1507–17.
27. Ding J, Li X, Hu H. TarPmiR: a new approach for microRNA target site prediction. Bioinformatics 2016;32:2768–75.
28. Chu C, Quinn J, Chang HY. Chromatin isolation by RNA purification (ChIRP). J Vis Exp 2012;61:3912.
29. Lin X, Zhuang S, Chen X, Du J, Zhong L, Ding J, et al. lncRNA ITGB8-AS1 functions as a ceRNA to promote colorectal cancer growth and migration through integrin-mediated focal adhesion signaling. Mol Ther 2022;30:688–702.
30. Castellanos-Rubio A, Fernandez-Jimenez N, Kratchmarov R, Luo X, Bhagat G, Green PH, et al. A long noncoding RNA associated with susceptibility to celiac disease. Science 2016;352:91–5.
31. D'Errico G, Machado HL, Sainz B Jr. A current perspective on cancer immune therapy: step-by-step approach to constructing the magic bullet. Clin Transl Med 2017;6:3.
32. Chung KY, Gore I, Fong L, Venook A, Beck SB, Dorazio P, et al. Phase II study of the anti-cytotoxic T-lymphocyte-associated antigen 4 monoclonal antibody, tremelimumab, in patients with refractory metastatic colorectal cancer. J Clin Oncol 2010;28:3485–90.
33. Brahmer JR, Drake CG, Wollner I, Powderly JD, Picus J, Sharfman WH, et al. Phase I study of single-agent anti-programmed death-1 (MDX-1106)

in refractory solid tumors: safety, clinical activity, pharmacodynamics, and immunologic correlates. J Clin Oncol 2010;28:3167–75.
34. Blaauboer A, Sideras K, van Eijck CHJ, Hofland LJ. Type I interferons in pancreatic cancer and development of new therapeutic approaches. Crit Rev Oncol Hematol 2021;159:103204.
35. Chawla-Sarkar M, Lindner DJ, Liu YF, Williams BR, Sen GC, Silverman RH, et al. Apoptosis and interferons: role of interferon-stimulated genes as mediators of apoptosis. Apoptosis 2003;8:237–49.
36. Sandoval R, Xue J, Pilkinton M, Salvi D, Kiyokawa H, Colamonici OR. Different requirements for the cytostatic and apoptotic effects of type I interferons. Induction of apoptosis requires ARF but not p53 in osteosarcoma cell lines. J Biol Chem 2004;279:32275–80.
37. Sangfelt O, Erickson S, Castro J, Heiden T, Gustafsson A, Einhorn S, et al. Molecular mechanisms underlying interferon-alpha-induced G_0–G_1 arrest: CKI-mediated regulation of G1 Cdk-complexes and activation of pocket proteins. Oncogene 1999;18:2798–810.
38. Fan JB, Miyauchi S, Xu HZ, Liu D, Kim LJY, Burkart C, et al. Type I interferon regulates a coordinated gene network to enhance cytotoxic T cell-mediated tumor killing. Cancer Discov 2020;10:382–93.
39. Le Bon A, Durand V, Kamphuis E, Thompson C, Bulfone-Paus S, Rossmann C, et al. Direct stimulation of T cells by type I IFN enhances the CD8+ T cell response during cross-priming. J Immunol 2006;176:4682–9.
40. Heidemann E, Weber J, Schmidt H, Reichmann U. Recombinant interferon alpha 2 stimulation of target-binding by natural killer cells. Klin Wochenschr 1986;64:1036–40.
41. Ito T, Amakawa R, Inaba M, Ikehara S, Inaba K, Fukuhara S. Differential regulation of human blood dendritic cell subsets by IFNs. J Immunol 2001;166:2961–9.
42. Ren Z, Ding T, Zuo Z, Xu Z, Deng J, Wei Z. Regulation of MAVS expression and signaling function in the antiviral innate immune response. Front Immunol 2020;11:1030.
43. Xu L, Peng L, Gu T, Yu D, Yao YG. The 3'UTR of human MAVS mRNA contains multiple regulatory elements for the control of protein expression and subcellular localization. Biochimica Biophys Acta Gene Regul Mech 2019;1862:47–57.
44. Yang Q, Li F, He AT, Yang BB. Circular RNAs: expression, localization, and therapeutic potentials. Mol Ther 2021;29:1683–702.
45. Kalbasi A, Ribas A. Tumour-intrinsic resistance to immune checkpoint blockade. Nat Rev Immunol 2020;20:25–39.